



Phase-change materials for energy-efficient photonic memory and computing

Wen Zhou,¹ Nikolaos Farmakidis, Johannes Feldmann, Xuan Li, James Tan, Yuhan He, C. David Wright, Wolfram H.P. Pernice, and Harish Bhaskaran*

Neuromorphic algorithms achieve remarkable performance milestones in tasks where humans have traditionally excelled. The breadth of data generated by these paradigms is, however, unsustainable by conventional computing chips. In-memory computing hardware aims to mimic biological neural networks and has emerged as a viable path in overcoming fundamental limitations of the von Neumann architecture. By eliminating the latency and energy losses associated with transferring data between the memory and central processing unit (CPU), these systems promise to improve on both speed and energy. Photonic implementations using on-chip, nonvolatile memories are particularly promising as they aim to deliver energy-efficient, high-speed, and high-density data processing within the photonic memory with the multiplexing advantages of optics. In this article, we overview recent progress in this direction that integrates phase-change material (PCM) memory elements with integrated optoelectronics. We compare performances of PCM devices using optoelectronic programming schemes and show that energy consumption can be significantly reduced to 60 pJ using picosecond (ps) optical pulse programming and plasmonic nanogap devices with a programming speed approaching 1 GHz. With these energy-efficient waveguide memories, concepts of in-memory photonic computing are implemented based on crossbar arrays. Compared with digital electronic accelerators: application-specific integrated circuits (ASICs) and graphics processing units (GPUs), photonic cores promise 1–3 orders higher compute density and energy efficiency, although much more work toward commercialization is still required.

Introduction

Advances in information technology have fueled rapid developments in AI, machine learning, big data, and the Internet of Things. Current growth rates in data traffic exceed 24% per year, while the data created and replicated are predicted to exceed 175 zettabytes (1 zettabyte = 10^{21} bytes) in 2025.¹ Coping with data of this magnitude has so far been addressed by employing large-volume memory and high-speed processor clusters, a strategy that is proving unsustainable based on

the projected requirements. The von Neumann architecture in particular, which makes up the foundation of modern computers, requires continuous data shuttling between the physically separated processing and memory units, a process where nearly two-thirds of the total energy is consumed.²

Inspired by biological neurons, in-memory computing architectures are gaining popularity, wherein data processing within or in the vicinity of memory units reduces latency and dissipation.³ Chalcogenide-based phase-change materials

Wen Zhou, Department of Materials, University of Oxford, Oxford, UK

Nikolaos Farmakidis, Department of Materials, University of Oxford, Oxford, UK

Johannes Feldmann, Department of Materials, University of Oxford, Oxford, UK

Xuan Li, Department of Materials, University of Oxford, Oxford, UK

James Tan, Department of Materials, University of Oxford, Oxford, UK

Yuhan He, Department of Materials, University of Oxford, Oxford, UK

C. David Wright, Department of Engineering, University of Exeter, Oxford, UK

Wolfram H. P. Pernice, Institute of Physics, University of Münster, Münster, Germany; Kirchhoff-Institute for Physics, Heidelberg University, Heidelberg, Germany;

Harish Bhaskaran, Department of Materials, University of Oxford, Oxford, UK; harish.bhaskaran@materials.ox.ac.uk

*Corresponding author

doi:10.1557/s43577-022-00358-7

(PCMs) widely used in rewriteable compact discs (CDs) and digital video discs (DVDs), are particularly well suited to achieve this task because the memory states of the material are nonvolatile and can be read out both optically and electrically.⁴ For an example, in a CD, binary data are stored by switching the PCM between its two structural phases (i.e., the disordered amorphous state (top) and the ordered crystalline state (bottom) illustrated in **Figure 1a**). Phase transitions can be triggered by heating up the PCMs with optical or electrical pulse stimuli. It allows precise tailoring of the optical and electrical properties of the materials. In the electronic domain, in-memory computing is achieved by storing analogue conductance values in the PCM cells, which are commonly arranged in a crossbar array.⁵ Implementations in the electronic domain, however, suffer from limitations in bandwidth and data throughput.

Addressing these limitations, photonic implementations of analogue in-memory photonic computing are projected to play a game-changing role in AI hardware. These systems leverage the ultrahigh bandwidth of optical interconnects,

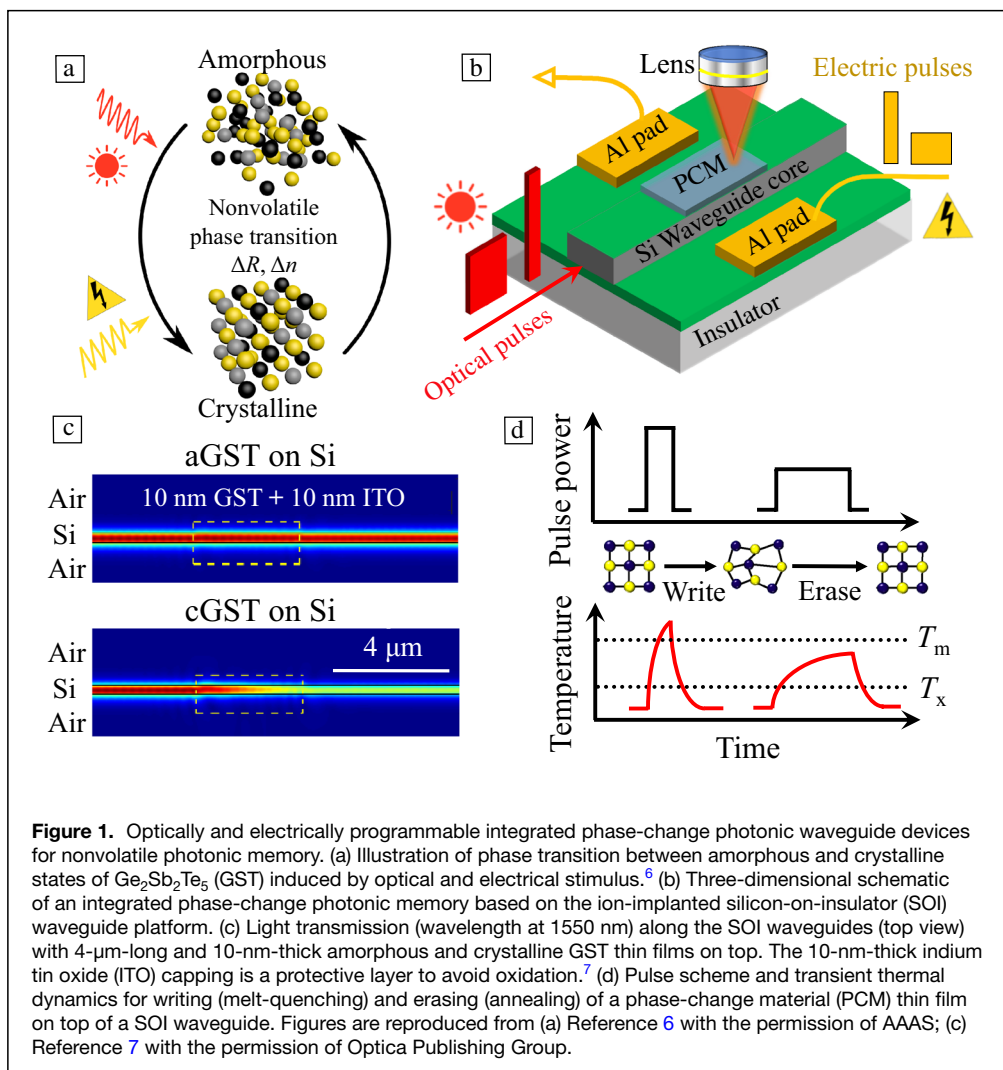
and data storage capacity of PCMs to collocate the memory and processing units and perform operations at the speed of light.⁸ Importantly, performing linear operations such as multiply accumulate (MAC) and matrix–vector multiplication (MVM) in the optical domain not only improves the speed, but also consumes considerably less energy.⁹ This results in favorable, sublinear scaling of energy consumption with respect to the number of operations for photonic hardware. Taken together, these properties lead to a significant increase in energy efficiency and compute power.

Working principle of optoelectronic waveguide memory cells

In the optical domain, transmission of light can be modulated by the structural phase transition of the PCM thin film deposited on top of an optoelectronic waveguide device (as shown in the schematic in **Figure 1b**).¹⁰ Specifically, a shallow-etched silicon photonic rib waveguide confines light with low transmission loss in its waveguide core, which consists of a silicon slab with a strip on it. However, a full-etched ridge waveguide

only has a strip on top of the insulator layer. The PCM while nearly lossless in its amorphous state, becomes absorptive upon phase transition to the crystalline state. **Figure 1c** shows simulated light transmission through a silicon waveguide with 4- μm -long and 10-nm-thick amorphous $\text{Ge}_2\text{Sb}_2\text{Te}_5$ (aGST) and crystallized $\text{Ge}_2\text{Sb}_2\text{Te}_5$ (cGST) as the PCM.⁷ Here, optical transmission is defined as the ratio between output and input optical intensity, which decreases from 95% in the case of aGST to 26% with cGST. In this optical memory cell, the signal information is stored as the PCM structural phase.

To switch the structural state of the PCM thin film, optical pulses (red) in the waveguide/free-space and electrical pulses (yellow) are sent to the photonic



waveguide memory cell. When an optical pulse is sent, the PCM thin film absorbs the optical energy and generates heat. When an electrical pulse is sent instead, the net current from the electrical pulse passes through an ion-implanted resistive region in a silicon waveguide, and thus generates heat.¹¹ Upon phase transition by pulse heating, the signal modulation (attenuation) induced by the different PCM states can be applied to mimic the workings of a biological synapse, which likewise, contain both synaptic plasticity modulation and memory functions.¹² The PCM states are highly stable for years at room temperature.^{10,13} Generally, a short and high-amplitude optical/electrical pulse is used to melt-quench (i.e., temperature sharply rising above the melting temperature (T_m) and quickly dissipates to room temperature) the PCM to an amorphous state as shown in Figure 1d. In contrast, a longer and lower amplitude optical/electrical pulse is used to anneal the PCM with temperature ramping up between T_m and transition temperature (T_x) for a certain period (to recrystallize the atomic lattice), before finally ramping the temperature down to room temperature. Specifically, T_x is 620–660 K with pulse time duration from 1 μ s down to 100 ns and T_m is ~900 K for GST.¹⁴

Optical programming of PCM waveguide devices

In 2012, the concept of nonvolatile photonic memories was first proposed.^{15,16} In 2013, Rudé et al. first demonstrated an on–off switch based on a silicon racetrack resonator by far-field free-space optical pulse switching of a GST patch on the ring as shown in Figure 2a.¹⁷ In an amorphous (crystalline) state, light is on (off) resonance and is filtered by (pass) the ring. Due to flexible programming on an arbitrary location, this approach based on free-space switching is widely used for patterning PCM metasurface devices for manipulating light scattering, deflection, and focusing.^{18,19} Recently, Delaney et al. demonstrated a reprogrammable 1×2 waveguide power splitter using digital patterning of ultralow-loss PCMs Sb_2S_3 and Sb_2Se_3 ²⁰ as shown in Figure 2b.²¹ By patterning phase states of a PCM, light propagating in the waveguide can be either equally split or routed to one of the output ports, which is promising for reconfigurable photonic circuits. However, a portion of the pump pulse passes through the thin PCM film in far-field free-space programming, which leads to relatively large energy consumption. For an example, energy of an amorphization pulse is at least 900 pJ.¹⁷

In contrast to free-space optical switching, sending pump pulses along the waveguide leads to in-plane light–PCM interaction with perfect absorption and reduced programming energies. In 2015, Ríos et al. developed an integrated multilevel waveguide memory (Figure 2c) using this optical near-field effect with switching energies as low as 13.4 pJ and speeds approaching 1 GHz.¹⁰ This fully integrated approach is more robust and reliable for practical applications without movable and bulky free-space optical components (deflection mirrors and lens) for focusing the pump pulses. Figure 2d shows switching dynamics of an amorphization event in an add-drop

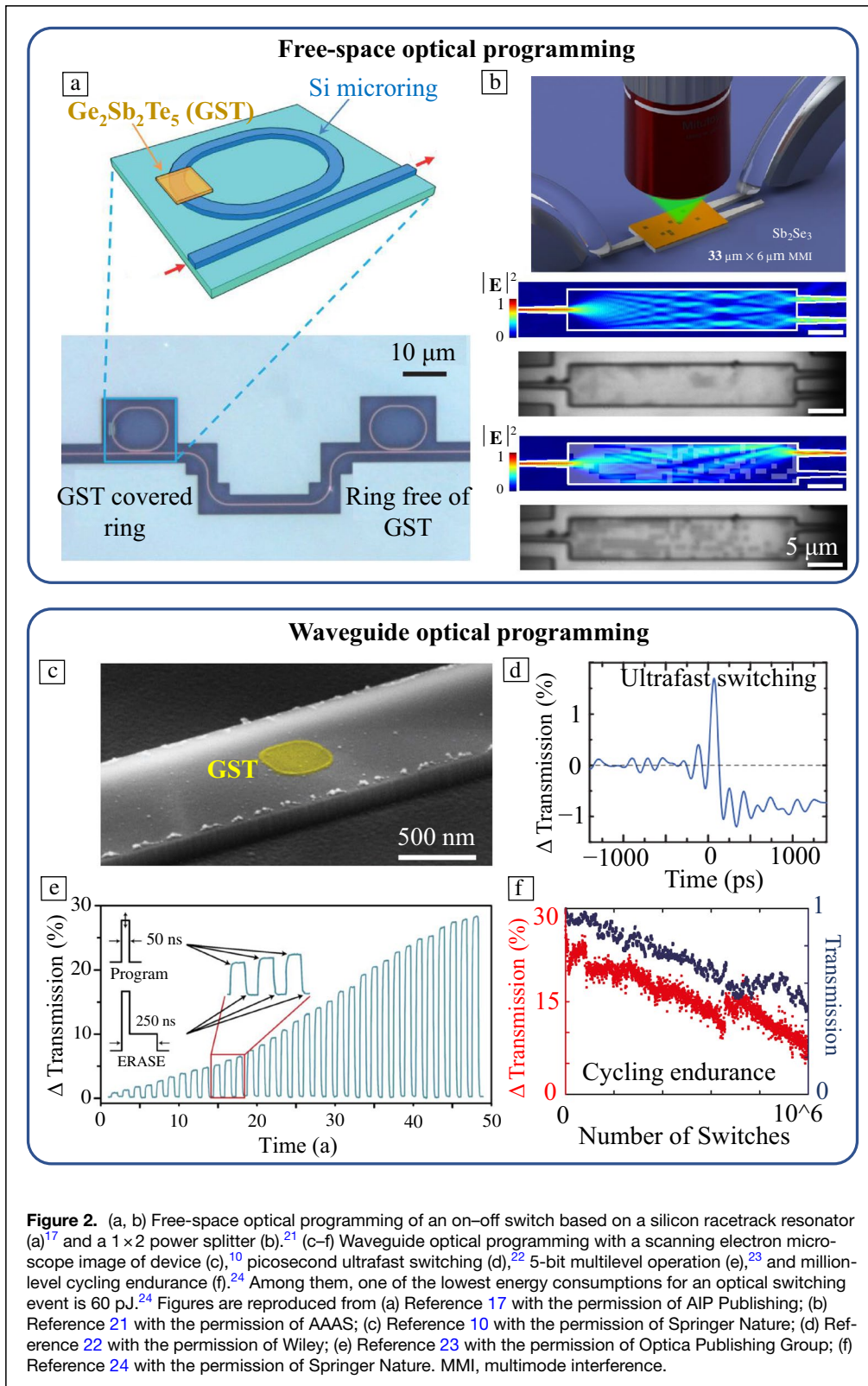
ring resonator triggered by a single 1-ps optical pulse. Rapid phase transition within 250 ps is probed.²² Multilevel programming was performed using pulse amplitude modulation, and a 5-bit (over 32 unique levels) nonvolatile photonic memory was demonstrated.²³ Note that a 6-bit waveguide memory was recently demonstrated using phase-change waveguide metasurfaces.²⁵ It also shows over 1-million cycling endurance.²⁴ These examples indicate that waveguide optical programming provides ultrafast, robust, multilevel, and energy-efficient operations.

Electrical programming of PCM waveguide devices

In addition to optical programming, electrical stimulus can also induce phase transition of PCMs based on Joule heating. In 2019, Zhang et al. developed an ion-implanted silicon waveguide microheater with a 1- μ m-wide P^{++} heavily doped strip region (black color) as shown in Figure 3a.¹¹ It shows 300% on–off switching contrast, and energy consumption of 10 nJ and 9 nJ for the amorphization and crystallization processes, respectively. The advantage of a microheater is electrical switching of low-loss $Ge_2Sb_2Se_4Te_1$ (GSST)²⁶ and lossless PCMs (Sb_2S_3 and Sb_2Se_3),²⁰ which is not easily achievable using optical switching due to extremely low absorption of pump light by PCMs. Figure 3b shows a reprogrammable and nonvolatile phase shifter based on a N-type-doped silicon waveguide microheater.²⁷ It shows phase modulation up to $0.09 \pi/\mu$ m and a low insertion loss of 0.3 dB/ π . A PIN diode microheater as shown in Figure 3c is developed to largely reduce insertion loss to 0.02 dB/ μ m because light is mainly confined in the intrinsic silicon region (i-Si) to avoid light absorption by free carriers.²⁸ Energy consumptions are 650 nJ and 11 nJ for the amorphization and crystallization processes, respectively. As for other waveguide platforms (e.g., SiC, Si_3N_4 , $LiNbO_3$) with large bandgaps, microheaters can be achieved by capping resistive ITO²⁹ and graphene strips³⁰ on top of waveguides to heat up PCMs as shown in Figure 3d–e, respectively. A recent study predicts that graphene microheaters display two orders of magnitude higher figure of merits (FOMs) for heating and overall performance compared with those of ITO and silicon PIN microheaters.³¹

Mixed-mode waveguide memory cells

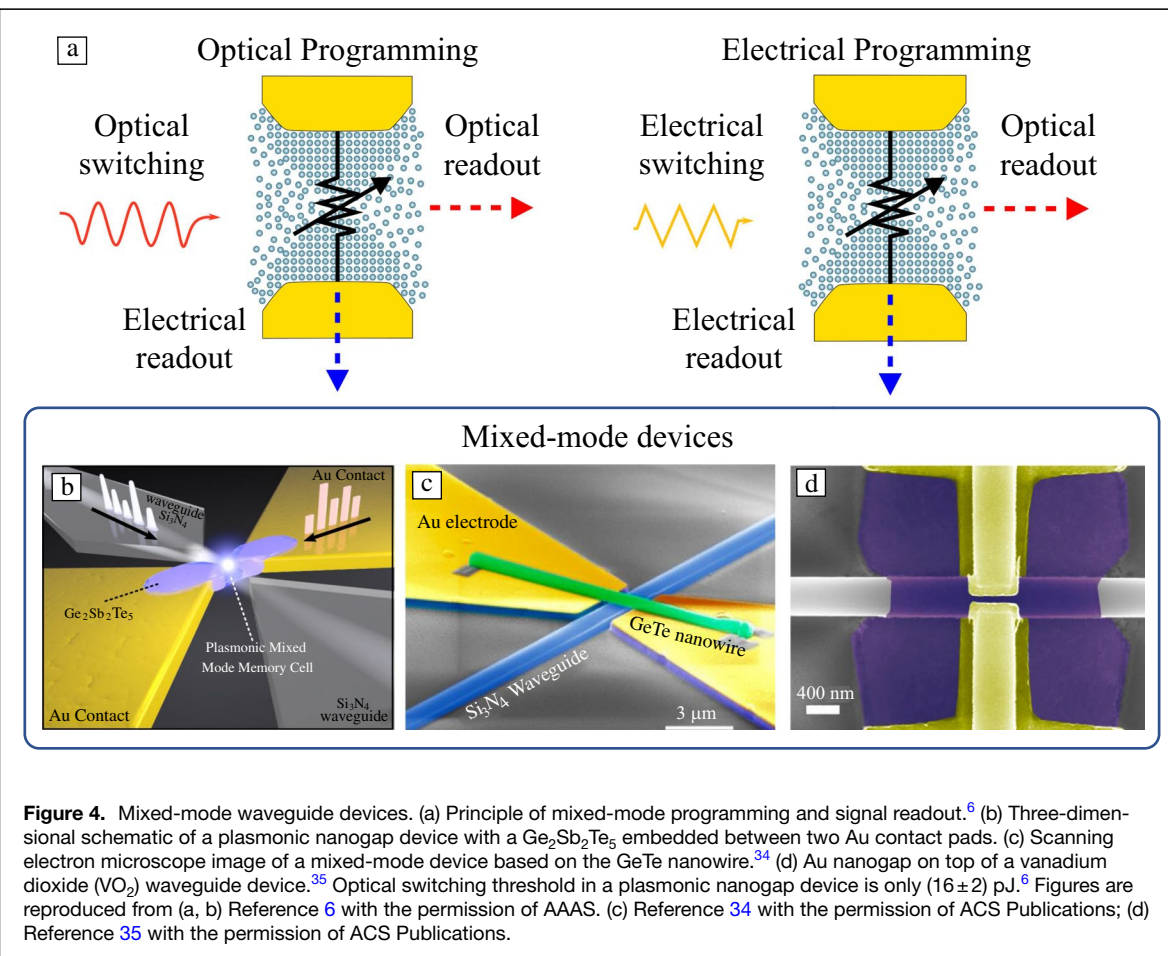
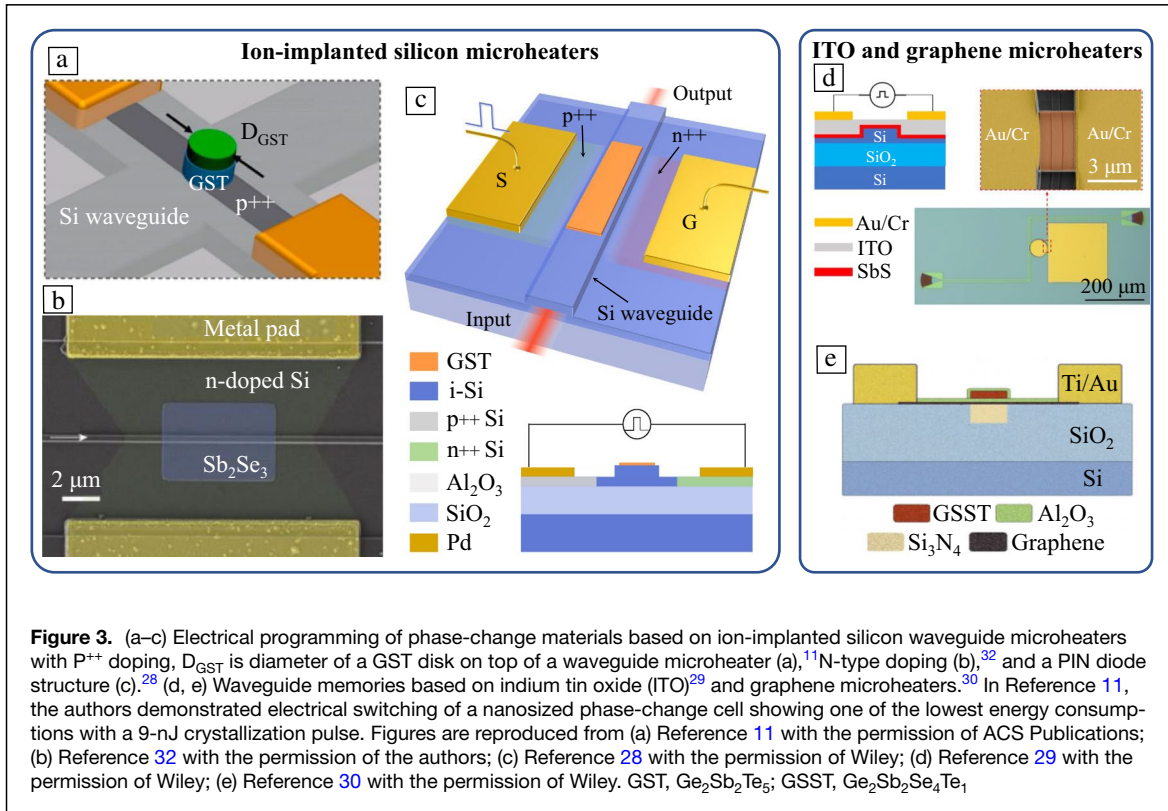
To be programmed and probed both optically and electrically, plasmonic nanogap devices support mixed-mode operation as a nonvolatile optoelectronic interface.⁶ Plasmonic nanogap devices in particular have been used to locally enhance light–matter interactions in the phase-change cell, thereby combining low energy programming and a small footprint. Here, the state of the PCM can be programmed using optical or electrical pulses and can be further read simultaneously in the optical and electrical domains. Its working principle is detailed in Figure 4a. Optical programming of the mixed-mode memory cell is based on the absorption of optical pulses



a conductive filament (cPCM) in a PCM element may be either formed or broken between the two gold pads based on either the threshold switching or Joule heating and subsequent melt-quenching of the cGST filament.³³ Figure 4b shows the 3D schematic of a plasmonic memory cell interfaced with input and output tapered photonic waveguides for enhanced optical signal delivery. A GST patch (blue) is placed between a 50-nm-wide gold nanogap. Switching energy required to initiate a phase transformation in the GST cell can be largely reduced due to extreme light intensity enhancement in the plasmonic nanogap due to excitation of surface plasmons polaritons (i.e., coupling of light with collective oscillations of the electrons at the surface of a metal). The size of the active region is 50 nm \times 50 nm in cross section. The gold nanogap also serves as electrical connections to probe the resistance change in the GST. As such, it supports mixed-mode operation, wherein electrical and optical signals can be employed to pump (switch) and probe (read) the device, with

any combination of the above. Optical switching threshold using the approach is only (16 ± 2) pJ. Figure 4c shows a mixed-mode device based on a GeTe nanowire suspended on

any combination of the above. Optical switching threshold using the approach is only (16 ± 2) pJ. Figure 4c shows a mixed-mode device based on a GeTe nanowire suspended on



top of a Si_3N_4 waveguide. GeTe nanowire can be optically switched using near-field evanescent coupling and probed both optically and electrically.³⁴ Figure 4d shows a VO_2 -based electro-optic modulator with optical and electrical probing of the semiconductor-to-metal phase transition in VO_2 .³⁵

Performance comparison of PCM devices

Table I summarizes performances of the state-of-the-art PCM devices using optical, electrical, and mixed-mode programming. Note that energy consumption can be reduced from nJ to pJ level using near-field waveguide optical switching instead of far-field free-space optical switching. One of the lowest energy consumptions (60 pJ/190 pJ) is achieved by using ps pump pulses with a relatively high switching contrast (20%) and a programming speed approaching GHz.²⁴ A mixed-mode nanogap device offers one of the lowest switching thresholds (16 ± 2 pJ).⁶ Thus, performances of photonic memory cells may be further improved by exploiting both plasmonic enhancement and ultrashort optical pulse programming. Electrical programming is also promising for achieving large contrasts (300%) with energy consumption of a few nJ.¹¹ In this scenario, a large area of PCM can be switched by a single electrical pulse. For an example, a patterned PCM metasurface with an area up to $0.4 \times 0.4 \text{ mm}^2$ was almost uniformly heated up and switched back and forth using microheaters.³⁶ Another advantage of using microheaters is flexible programming of low-loss/lossless PCMs (GSST, Sb_2S_3 , Sb_2Se_3).

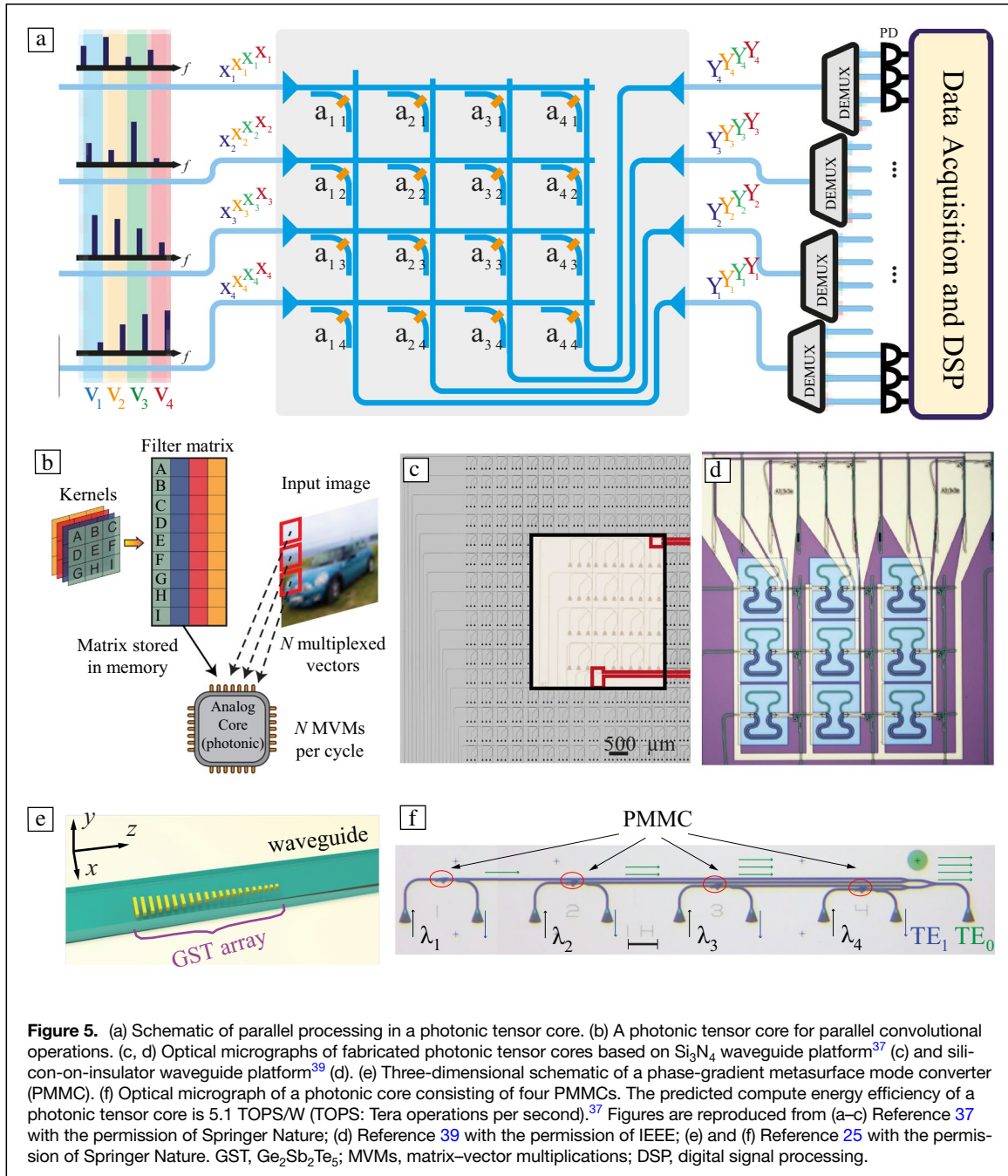
In-memory photonic tensor core

Based on the previously discussed energy-efficient optoelectronic waveguide memory cells, the development of large-scale memory chips is more promising as these photonic

memory cells can be used to implement in-memory computing, such as a photonic tensor core for performing multiply accumulate (MAC) operations and matrix-vector multiplications (MVMs) using photonic integrated circuits. A matrix with $m \times n$ weight banks can be represented on a hardware in the form of a photonic crossbar array (illustrated in **Figure 5a**).³⁷ Output pulse intensity ($c = a \times b$) through a PCM can be calculated using multiplication between PCM transmittance (a) and input pulse intensity (b).³⁸ Collected light intensity (Y_i) at each output port using the incoherent superposition is basically a series of MAC operations (i.e., a dot product of a vector (X_1, X_2, \dots, X_m) encoded in the input pulse intensities and a vector ($a_{1i}, a_{2i}, \dots, a_{mi}$) (kernel i) stored in the transmission value of the memory cells). Thus, MAC and MVM operations are achieved by collecting summation of modulated optical intensity at each output port and all output ports of a crossbar array, respectively. Four sets of vectors (X_1, X_2, X_3, X_4) (labeled with different colors) can be encoded on light intensities with 16 discrete wavelengths. At the output ports of the tensor core, wavelength demultiplexers (DEMUXs) are used to only separate a single-wavelength channel into one output path for detecting each Y_i . This allows emulation of massively parallel processing in neural networks. As illustrated in **Figure 5b**, parallel processing of several images (indicated by three red frames) and one kernel simultaneously based on WDM is a huge advantage of photonic architectures compared with serial information processing in the digital computer. This results in high computational density and efficiency with low latency as multiple MVMs are performed in a single clock cycle. **Figure 5c** shows an optical micrograph of a photonic tensor core based on SiN waveguides with a mesh of 16×16 fabricated in the cleanroom using electron-beam lithography

Table I. Experimentally characterized performances of the state-of-the-art PCM devices.

	Thickness of PCM and Substrate	Pulse Widths (crystallization/amorphization)	Energies (crystallization/amorphization)	Change in Transmission/Reflection (%)	References
Free-space optical programming	20-nm GST on SOI	300 ns/20 ns	3.6 nJ/0.9 nJ	Extinction ratio (ER) = 12 dB	17
	70-nm GST on glass substrate	85 fs (80 pulses)/85 fs	31.2 nJ/1.25 nJ	~95%	18
	75-nm GST-326 on alumina antenna	450 ns/450 ns	3.15 nJ /15.75 nJ	233.3%	19
	40-nm Sb_2Se_3 on silicon substrate	100 ms/400 ns	9 mJ/36 nJ	~100%	20
Waveguide optical programming	10-nm GST on SiN	700 ns/100 ns	3.1 nJ/533 pJ	21%	10
	10-nm AgInSbTe on SiN	5 ps/10 ps	60 pJ/190 pJ	20%	24
	20-nm GST on SiN	600 ps/2 ps	17 nJ/190 pJ	ER = 6 dB	22
	10-nm GST on SiN	250 ns/50 ns	680 pJ/135 pJ	28%	23
	10-nm GST on SOI	625 ns/100 ns	15.6 nJ/380 pJ	15%	7
Electrical programming	30-nm GST on SOI	100 ns/20 ns	9 nJ/10 nJ	300%	11
	10/20-nm GST on SOI	80 μs /100 ns	715 nJ/ 13 nJ	50%	28
	30-nm Sb_2Se_3 on SOI	1 ms/400 ns	38.4 μJ / 176 nJ	ER = 20 dB	32
	30-nm GSST on SOI	20 ms/50 μs	0.23 mJ/1.2 μJ	ER = 8 dB	27
	230-nm GSST on TiPt heaters	500 ms/5 μs	2.5 J/100 μJ	400%	36
Mixed-mode programming	GeTe nanowire on SiN	50 ns/50 ns	6.2 nJ/8 nJ	15%	34
	75-nm GST-225 on Au nanogap	408 ns/8 ns	1.26 nJ/60 pJ	4%	6



and reactive ion etching.³⁷ Figure 5d shows an optical micrograph of a photonic tensor core based on SOI waveguides with a mesh of 3×3 fabricated by multi-project wafer (MPW) service.³⁹ Recently, Wu et al. proposed a phase-gradient metasurface mode converter (PMMC) as shown in Figure 5e for mode conversion from the fundamental mode to the 1st-order mode. As shown in Figure 5f, a MAC core is realized with four inputs biased by weights setting of PMMCs.²⁵ Compute density and compute efficiency are, respectively, predicted to be 880 TOPS/ mm^2 and 5.1 TOPS/W for a 64×64 crossbar-based photonic tensor core operating at 25-GHz clock speed.

Compared with digital electronic accelerator (ASIC and GPU), the photonic core has 1–3 orders of magnitude improvement in both compute density and efficiency. Detailed estimation can be found in Reference 37.

Summary

In summary, we have overviewed recent progress in the development of energy-efficient waveguide memory cells for applications in in-memory and neuromorphic photonic computing. Waveguide memory cells leverage the near-field interaction to reduce energy consumption. Crucially, energy

consumption is only 60 pJ in an all-optical abacus with operating speed approaching 1 GHz.²⁴ And optical switching threshold is drastically reduced to (16 ± 2) pJ in a plasmonic nanogap device.⁶ High-performance waveguide memory cells have been deployed to achieve neuromorphic^{40,41} and in-memory computing.³⁸ When used as a neuromorphic tensor core, it is scalable for various AI applications, for example to enable edge detection capabilities via convolutional filter and linear transformation as a fully connected layer in artificial neural networks.³⁷ The PCM memory is fully passive after nonvolatile weight setting. In addition, it has a large data throughput using parallel processing based on the WDM. Compared with digital electronic accelerators (ASIC and GPU), photonic cores show 1–3 orders of magnitude improvement in both compute density and efficiency.³⁷

Acknowledgments

The authors acknowledge funding from the EU H2020 Program (Grant No. 780848, Fun-COMP Project). We would also like to thank the many members of our research groups, and external collaborators, whose remarkable efforts generated much of the research results described in this article.

Conflict of interest

On behalf of all authors, the corresponding author states that there is no conflict of interest.

Open Access

This article is licensed under a Creative Commons Attribution 4.0 International License, which permits use, sharing, adaptation, distribution and reproduction in any medium or format, as long as you give appropriate credit to the original author(s) and the source, provide a link to the Creative Commons license, and indicate if changes were made. The images or other third party material in this article are included in the article's Creative Commons license, unless indicated otherwise in a credit line to the material. If material is not included in the article's Creative Commons license and your intended use is not permitted by statutory regulation or exceeds the permitted use, you will need to obtain permission directly from the copyright holder. To view a copy of this license, visit <http://creativecommons.org/licenses/by/4.0/>.

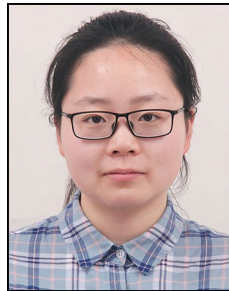
References

1. D. Reinsel, J. Gantz, J. Rydning, I.D.C. Report, *The Digitization of the World From Edge to Core* (International Data Corporation, Framingham, MA, 2018)
2. A. Boroumand, S. Ghose, Y. Kim, R. Ausavarungnirun, E. Shiu, R. Thakur, D. Kim, A. Kuusela, A. Knies, P. Ranganathan, O. Mutlu, *ACM SIGPLAN Notices* **53**, 316 (2018)
3. A. Sebastian, M. Le Gallo, R. Khaddam-Aljameh, E. Eleftheriou, *Nat. Nanotechnol.* **15**, 529 (2020)
4. W. Zhang, R. Mazzarello, E. Ma, *MRS Bull.* **44**(9), 686 (2019)
5. S. Raoux, D. Ielmini, M. Wuttig, I. Karpov, *MRS Bull.* **37**(2), 118 (2012)
6. N. Farmakidis, N. Youngblood, X. Li, J. Tan, J.L. Swett, Z.G. Cheng, C.D. Wright, W.H.P. Pernice, H. Bhaskaran, *Sci. Adv.* **5**, eaaw2687 (2019)

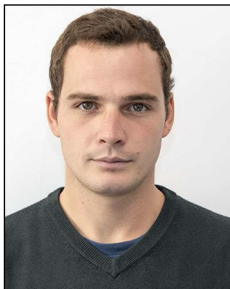
7. X. Li, N. Youngblood, Z. Cheng, S. Carrillo, E. Gemo, W.H.P. Pernice, C.D. Wright, H. Bhaskaran, *Optica* **7**, 218 (2020)
8. C.D. Wright, H. Bhaskaran, W.H.P. Pernice, *MRS Bull.* **44**(9), 721 (2019)
9. B.J. Shastri, A.N. Tait, T.F.D. Lima, W.H.P. Pernice, H. Bhaskaran, C.D. Wright, P.R. Prucnal, *Nat. Photonics* **15**, 102 (2021)
10. C. Rios, M. Stegmaier, P. Hosseini, D. Wang, T. Scherer, C.D. Wright, H. Bhaskaran, W.H.P. Pernice, *Nat. Photonics* **9**, 725 (2015)
11. H. Zhang, L. Zhou, L. Lu, J. Xu, N. Wang, H. Hu, B.M.A. Rahman, Z. Zhou, J. Chen, *ACS Photonics* **6**, 2205 (2019)
12. Z. Cheng, C. Rios, W.H.P. Pernice, C.D. Wright, H. Bhaskaran, *Sci. Adv.* **3**, e1700160 (2017)
13. M. Wuttig, N. Yamada, *Nat. Mater.* **6**, 824 (2007)
14. Z. Cheng, C. Rios, N. Youngblood, C.D. Wright, W.H.P. Pernice, H. Bhaskaran, *Adv. Mater.* **30**, 1802435 (2018)
15. W.H.P. Pernice, H. Bhaskaran, *Appl. Phys. Lett.* **101**, 171101 (2012)
16. J. Pello, J.J.G.M. van der Tol, M. Rude, R. Simpson, S. Keyvaninia, G. Roelkens, M.K. Smit, V. Pruneri, *16th European Conference on Integrated Optics and Technical Exhibition (ECIO)* (Barcelona, Spain, 2012)
17. M. Rudé, J. Pello, R.E. Simpson, J. Osmond, G. Roelkens, J.J.G.M. van der Tol, V. Pruneri, *Appl. Phys. Lett.* **103**, 141119 (2013)
18. Q. Wang, E.T.F. Rogers, B. Gholipour, C.-M. Wang, G. Yuan, J. Teng, N.I. Zheludev, *Nat. Photonics* **10**, 60 (2016)
19. A.-K.U. Michel, A. Heßler, S. Meyer, J. Pries, Y. Yu, T. Kalix, M. Lewin, J. Hanss, A. De Rose, T.W.W. Maß, M. Wuttig, D.N. Chigrin, T. Taubner, *Adv. Mater.* **31**, 1901033 (2019)
20. M. Delaney, I. Zeimpekis, D. Lawson, D.W. Hewak, O.L. Muskens, *Adv. Funct. Mater.* **30**, 2002447 (2020)
21. M. Delaney, I. Zeimpekis, H. Du, X. Yan, M. Banakar, D.J. Thomson, D.W. Hewak, O.L. Muskens, *Sci. Adv.* **7**, eabg3500 (2021)
22. M. Stegmaier, C. Rios, H. Bhaskaran, C.D. Wright, W.H.P. Pernice, *Adv. Opt. Mater.* **5**, 1600346 (2017)
23. X. Li, N. Youngblood, C. Rios, Z.G. Cheng, C.D. Wright, W.H.P. Pernice, H. Bhaskaran, *Optica* **6**, 1 (2019)
24. J. Feldmann, M. Stegmaier, N. Gruhler, C. Rios, H. Bhaskaran, C.D. Wright, W.H.P. Pernice, *Nat. Commun.* **8**, 1256 (2017)
25. C. Wu, H. Yu, S. Lee, R. Peng, I. Takeuchi, M. Li, *Nat. Commun.* **12**, 96 (2021)
26. Y. Zhang, J.B. Chou, J. Li, H. Li, Q. Du, A. Yadav, S. Zhou, M.Y. Shalaginov, Z. Fang, H. Zhong, C. Roberts, P. Robinson, B. Bohlin, C. Rios, H. Lin, M. Kang, T. Gu, J. Warner, V. Liberman, K. Richardson, J. Hu, *Nat. Commun.* **10**, 4279 (2019)
27. C. Rios, Q. Du, Y. Zhang, M. Shalaginov, P. Miller, P. Robinson, C. Roberts, M. Kang, K.A. Richardson, T. Gu, S. Vitale, J. Hu, *Conference on Lasers and Electro-Optics (CLEO)* (San Jose, CA, 2021), paper JTu2P.2
28. J. Zheng, Z. Fang, C. Wu, S. Zhu, P. Xu, J.K. Doylend, S. Deshmukh, E. Pop, S. Dunham, M. Li, A. Majumdar, *Adv. Mater.* **32**, 2001218 (2020)
29. Z. Fang, J. Zheng, A. Saxena, J. Whitehead, Y. Chen, A. Majumdar, *Adv. Opt. Mater.* **9**, 2002049 (2021)
30. C. Rios, Y. Zhang, M. Shalaginov, S. Deckoff-Jones, H. Wang, S. An, H. Zhang, M. Kang, K.A. Richardson, C. Roberts, J.B. Chou, V. Liberman, S.A. Vitale, J. Kong, T. Gu, J. Hu, *Adv. Photonics Res.* **2**, 2000034 (2021)
31. J. Zheng, S. Zhu, P. Xu, S. Dunham, A. Majumdar, *ACS Appl. Mater. Interfaces* **12**, 21827 (2020)
32. C. Rios, Q. Du, Y. Zhang, C.-C. Popescu, M. Y. Shalaginov, P. Miller, C. Roberts, M. Kang, K.A. Richardson, T. Gu, S.A. Vitale, J. Hu, <https://arxiv.org/2105.06010> (2021)
33. M.L. Gallo, A. Sebastian, *J. Phys. D Appl. Phys.* **53**, 213002 (2020)
34. Y. Lu, M. Stegmaier, P. Nukala, M.A. Giambra, S. Ferrari, A. Busacca, W.H.P. Pernice, R. Agarwal, *Nano Lett.* **17**, 150 (2017)
35. P. Markov, R.E. Marvel, H.J. Conley, K.J. Miller, R.F. Haglund, S.M. Weiss, *ACS Photonics* **2**, 1175 (2015)
36. Y. Zhang, C. Fowler, J. Liang, B. Azhar, M.Y. Shalaginov, S. Deckoff-Jones, S. An, J.B. Chou, C.M. Roberts, V. Liberman, M. Kang, C. Rios, K.A. Richardson, C. Rivero-Baleine, T. Gu, H. Zhang, J. Hu, *Nat. Nanotechnol.* **16**, 661 (2021)
37. J. Feldmann, N. Youngblood, M. Karpov, H. Gehring, X. Li, M. Stappers, M.L. Gallo, X. Fu, A. Lukashchuk, A. Raja, J. Liu, D. Wright, A. Sebastian, T. Kippenberg, W. Pernice, H. Bhaskaran, *Nature* **589**, 52 (2021)
38. C. Rios, N. Youngblood, Z.G. Cheng, M. Le Gallo, W.H.P. Pernice, C.D. Wright, A. Sebastian, H. Bhaskaran, *Sci. Adv.* **5**, eaau5759 (2019)
39. X. Li, N. Youngblood, W. Zhou, J. Feldmann, J. Swett, S. Aggarwal, A. Sebastian, C.D. Wright, W. Pernice, H. Bhaskaran, presented at the IEEE International Electron Devices Meeting (IEDM) (San Francisco, 2020)
40. N. Farmakidis, N. Youngblood, J.S. Lee, J. Feldmann, A. Lodi, X. Li, S. Aggarwal, W. Zhou, L. Bogani, W.H.P. Pernice, C.D. Wright, H. Bhaskaran, *Adv. Sci.* **9**, 2200383 (2022). <https://doi.org/10.1002/adv.202200383>
41. W. Zhou, N. Farmakidis, X. Li, J. Tan, S. Aggarwal, J. Feldmann, F. Brücknerhoff-Plückelmann, C.D. Wright, W.H.P. Pernice, H. Bhaskaran, *Phys. Status Solidi Rapid Res. Lett.* **16**, 2100487 (2022). <https://doi.org/10.1002/pssr.202100487> □



Wen Zhou is a postdoctoral researcher supported by the EU Horizon 2020 Fun-COMP Project at the University of Oxford, UK. He received his PhD degree in electronic engineering from The Chinese University of Hong Kong in 2018. He was a postdoctoral fellow supported by the Hong Kong Postdoctoral Hub—Innovation and Technology Fund from September 2018 to June 2019. His research interests include silicon photonics, phase-change materials, and in-memory photonic computing. Zhou can be reached by email at wen.zhou@materials.ox.ac.uk.



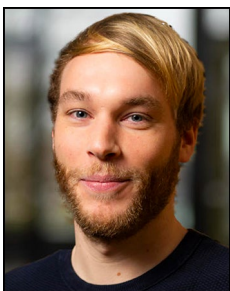
Yuhan He is currently a DPhil student, funded by the Microsoft Research PhD Scholarship Programme in Europe, Middle East & Africa, working on integrated photonics for neuromorphic applications. She received her BEng degree (2020) in electronic engineering from Tsinghua University, China. She was an intern at the University of Oxford, UK, in 2019, and an exchange student at Delft University of Technology, The Netherlands, from 2018 to 2019. He can be reached by email at yuhan.he@materials.ox.ac.uk.



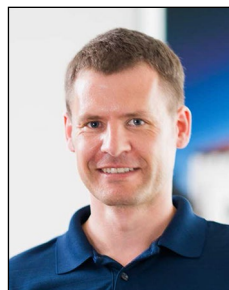
Nikolaos Farmakidis is an Engineering and Physical Sciences Research Council funded postdoctoral researcher in the Advanced Nanoscale Engineering Group at the University of Oxford, UK, where he was also a doctoral candidate. His research focuses on integrated photonics, plasmonics, and nanomanufacturing. Before joining the University of Oxford, he worked on micro- and nanofluidics and is the author of several scientific papers. Farmakidis can be reached by email at nikolaos.farmakidis@materials.ox.ac.uk.



C. David Wright is a professor of electronic and computer engineering at the University of Exeter, head of the Nano Engineering Science and Technology Group, and co-director of the University's Centre for Metamaterial Research and Innovation and its Engineering and Physical Sciences Research Council Centre for Doctoral Training in Metamaterials. He graduated with a BSc degree in physics from Imperial College of Science and Technology, UK. After working as a process engineer for Philips Electronics, he returned to academia, obtaining his MSc degree in solid-state physics from The University of Sheffield and a PhD degree in perpendicular magnetic recording from The University of Manchester. He held faculty positions at The University of Manchester, in both its Department of Electrical Engineering and its School of Computer Science, before taking up the Chair at Exeter in 1999. He is a Fellow of the UK Institution of Engineering Technology and a member of the IEEE. Wright's research centers on the development of future generation, nonvolatile, memory, and computing devices and technologies; and active optical metasurfaces for the control of light from the UV to the THz. Wright can be reached by email at david.wright@exeter.ac.uk.



Johannes Feldmann was a postdoctoral researcher at the University of Oxford, UK. He received his BS (2013) and MS (2015) degrees in physics from the WWU Münster, Germany. Feldmann then received his PhD degree at the University of Münster, Germany. His research is focused on the development of integrated nanophotonic circuits with phase-change materials for all-optical signal processing and computation, especially for artificial intelligence applications. He is a co-founder of Saliency Labs Ltd, a spin-out from the universities of Oxford and Münster, which he is working for since October 2021. Feldmann can be reached by email at johannes.feldmann@materials.ox.ac.uk.



Wolfram H.P. Pernice is a professor of physics at the University of Heidelberg, Germany. He was previously a professor of physics and also the deputy director of the Physics Institute and managing director of the Münster Nanofabrication Facility, Germany. He received his PhD degree from the University of Oxford, UK, after which he carried out postdoctoral research as a Humboldt Fellow at Yale University. Pernice's research interests include nanophotonics and optomechanics. He is a member of the German Young Academy of the Berlin-Brandenburg Academy of Sciences and Humanities and the German National Academy of Sciences Leopoldina. He is a co-founder of Saliency Labs Ltd and Pixel Photonics. Pernice can be reached by email at wolfram.pernice@uni-muenster.de.



Xuan Li received her PhD (2021) at the University of Oxford, UK. Her research focuses on neuromorphic computing with photonics and phase-change materials. Li can be reached by email at xuan.li@materials.ox.ac.uk.



Harish Bhaskaran is a professor of applied nanomaterials at the University of Oxford, UK. He obtained his BE degree from the University of Pune, India, and his MS and PhD degrees from the University of Maryland. Before joining Oxford, he was employed at IBM Research—Zurich, Switzerland, Yale University, and the University of Exeter, UK. His research focuses on data storage and computing devices, nanomechanics, and nanomanufacturing. He is the co-founder and chief scientific officer of Bodle Technologies Ltd. and a co-founder of Saliency Labs Ltd. Bhaskaran can be reached by email at harish.bhaskaran@materials.ox.ac.uk.



James Tan received his BS degree from University of Malaya and the MSc. degree in electrical engineering from the Korea Advanced Institute of Science and Technology. He then received his PhD degree at the University of Oxford, UK. His research is focused on the development of integrated optical circuits for artificial intelligence computations. Tan can be reached by email at james.tan@materials.ox.ac.uk.